You et al. Nanoscale Research Letters (2017) 12:360
DOI 10.1186/s11671-017-2139-0

Nanoscale Research Letters

NANO EXPRESS Open Access

Colorimetric Humidity Sensors Based on Electrospun Polyamide/$CoCl_2$ Nanofibrous Membranes

Ming-Hao You[1], Xu Yan[1,2*], Jun Zhang[1], Xiao-Xiong Wang[1], Xiao-Xiao He[1], Miao Yu[1,3], Xin Ning[2] and Yun-Ze Long[1,2*]

Abstract

Humidity indicators based on composite polyamide 66/cobalt chloride (PA66/$CoCl_2$) nanofibrous membranes (NFMs) were successfully fabricated by electrospinning. A series of NFMs with various weight percentage of $CoCl_2$ to PA66 were prepared, and their humidity sensitivity based on color changing and quartz crystal microbalance (QCM) were studied. Due to the color change property of cobalt chloride, the as-spun composite NFMs show obviously macroscopic color change from blue to pink as relative humidity (RH) increasing from 12.4 to 97.2%. Moreover, the QCM detection showed a linear dependence on the RH changing and exhibited short response/recovery time (less than 65.4 s/11 s), small hysteresis (less than 11%), good reproducibility, and stability. Owing to the above double sensitive mechanism on RH, the PA66/$CoCl_2$ composite NFM may show great potential applications from meticulous to coarse.

Keywords: Colorimetric humidity sensor, Electrospinning, PA66/$CoCl_2$ nanofibrous membranes

Background

Relative humidity (RH) sensor is mainly used for monitoring atmospheric humidity environment and shows important applications in warehousing [1], environmental monitoring [2], instruments and meters, and meteorology [3]. Until now, various types of humidity sensors have been reported, such as resistance type [4], capacitor type [5], field-effect-transistor type [6], optical type [7, 8], and so on. Among these types of sensors, the optical type has attracted a lot of interests since it is supplying a change in optical properties, easily detectable with the naked eye (visual) which is suitable for applications in daily life [8–10].

It is now believed that RH sensors based on the electrospun nanofibrous membranes (NFMs) show improved sensor sensitivity due to their large surface area to volume ratio [11–13], providing an increased number of sites for analyte interaction or signal transduction [10, 14–17]. For example, electrospun polyamide 6 nano-fiber/net modified by polyethyleneimine was investigated as RH indicator detected by quartz crystal microbalance (QCM) [14]. It shows high sensitivity and the response and recover times are 120 and 50 s, respectively, with RH changing from 2 to 35% [14]. Moreover, ceramic LiCl-doped ZnO electrospun fibers were also fabricated as humidity sensor, with response time and recovery time about 3 and 6 s [15].

While the sensitivity of the above humidity sensors based on electrospun fibers were detected by precise instrument, [14, 15] it may do not work in practical application limits to conditions. Optical humidity sensors will be a possible solution. Since RH do not have measurable intrinsic optical properties, some intermediate agent will be introduced to show a change in optical property. At present, several intermediate agents have been adapted to realize colorimetric indicator for humidity including photonic crystal [8, 9, 18], polymer electrolyte thin films [19], doped cholesteric liquid crystal [20], and crystalline covalent organic framework nanofibers [21]. In addition, cobalt chloride has been applied as colorimetric RH indicator for its color changes when contaminated by

* Correspondence: yanxu-925@163.com; yunze.long@163.com; yunze.long@qdu.edu.cn
[1]Collaborative Innovation Center for Nanomaterials & Devices, College of Physics, Qingdao University, Qingdao 266071, China
Full list of author information is available at the end of the article

water [7]. Typical colorimetric RH indicator such as silica gel self indicator and $CoCl_2$-based optical humidity sensor [7, 22] have been presented. However, colorimetric humidity sensor based on electrospun fibers was rarely investigated.

In this work, we fabricated PA66/cobalt chloride NFMs by electrospinning and investigated its humidity sensing properties by extensive color change and both fine quartz crystal microbalance (QCM). The results showed that the electrospun PA66/cobalt chloride NFM sensors exhibiting high humidity sensitivity with obviously color change, rapid response/recovery performance, small hysteresis, excellent reproducibility, and good stability.

Methods

Preparation of Polymer/Cobalt Chloride Solutions

The solutes were $CoCl_2{\cdot}6H_2O$ (Sinopharm Chemical Reagent Co., Ltd) and PA66 (Tianjin Heowns Biochem LLC., China). As a comparison, the concentrations of $CoCl_2{\cdot}6H_2O$ in these solutes were 0 (pure PA66), 10, 30, and 50 wt%, respectively. Dissolved these solutes in formic acid at 12 wt% and stirred thoroughly for 6 h at room temperature, then the uniform precursor solutions were obtained.

Fabrication of Colorimetric Nanofiber Membranes for Humidity Detection

The process of fabricating fiber membranes by electrospinning is depicted in Fig. 1a. Firstly, the precursor solution was loaded into a syringe and regulated the flow rate of the solution at 10 μL min^{-1} by a syringe pump (LSP01-1A, Baoding Longer Precision Pump Co., Ltd., China). The applied voltage was kept at 18 kV, and the distance between the needle and collector was about 15 cm. The ambient humidity was controlled at 50–60% RH, and the temperature was between 20 and 25 °C. Electrospinning for about 30 min, the as-spun composite NFMs could be obtained.

Fabrication of Sensing Membranes on QCM

To further investigate the humidity sensitivity of the as-spun NFM, we also selected QCM for precision measurement. The process of fabricating sensing NFMs on the QCM (CHI400C, Shanghai Huachen Instruments Co., Ltd., China) chip is showed in Fig. 1b. Under the above electrospinning conditions, PA66/cobalt chloride NFMs were deposited onto the surface of the QCM chip, and then the humidity sensitivity can be measured.

Characterization

The photographs of the colorimetric NFMs were recorded by a digital camera (DSC-TX9C 50i). Absorption spectra were recorded by a UV-vis spectrometer (U-4100, Hitachi) under absorption mode. The morphologies and structures of the NFMs were characterized by a scanning electron microscopy (SEM, EVO MA 10/LS 10, CARL ZEISS Co., Ltd., Germany) and a transmission electron microscope (TEM, JEM-2100PLUS, JEOL Ltd., Japan). Fourier transform infrared (FT-IR) spectra were recorded on a Thermo Scientific Nicolet In10 spectrometer. Means for humidity control are saturated salt solution humidity bottles, which have a stable humidity environments of 12.4% RH (Saturated LiCl solution, in 20 °C), 33.6% RH (Saturated $MgCl_2$ solution, in 20 °C), 55.2% RH (Saturated $Na_2Cr_2O_7{\cdot}2H_2O$ solution, in 20 °C), 75.5% RH (Saturated NaCl solution, in 20 °C), and 97.2% RH (Saturated K_2SO_4 solution, in 20 °C), respectively.

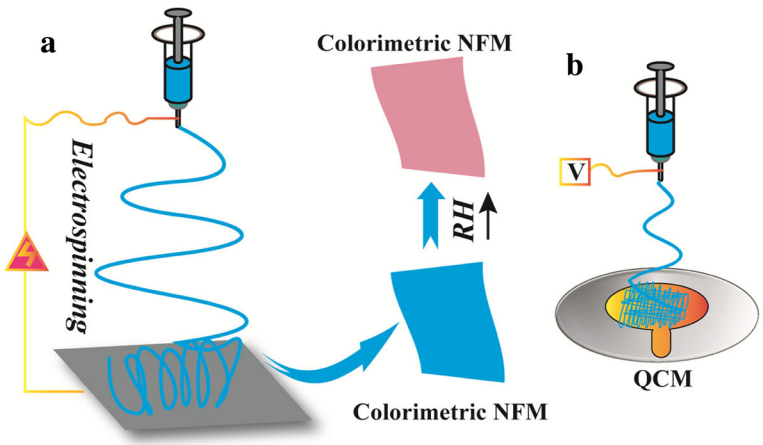

Fig. 1 Schematic illustrations of the electrospinning process to fabricate hybrid PA66/cobalt chloride NFM. **a** Fabrications of colorimetric NFM for humidity detection. **b** Illustration of depositing NFMs on the electrode surface of the QCM

Results and Discussion

Colorimetric Property of the As-Spun NFM upon Exposure to Humidity

Figure 2a shows the color changes of the electrospun PA66/$CoCl_2$ NFMs with different concentrations of $CoCl_2{\cdot}6H_2O$ NFMs exposure to different RH. As can be seen that the color of pure PA66 NFM is white, while the colors of PA66/$CoCl_2$ NFMs in low humidity are blue, and as the concentration of cobalt chloride changed from 10 to 50 wt%, the color of the PA66/$CoCl_2$ NFM became more and more concentrated. As humidity increases, especially for 50 wt% $CoCl_2{\cdot}6H_2O$ NFM, the blue color of the NFM gradually fades and turns to pink in the 97.2% RH.

In order to ensure the colors of PA66/cobalt chloride NFM exposed to different relative humidity conditions, visible absorption spectra (380–780 nm) of the 50 wt% $CoCl_2{\cdot}6H_2O$-doped NFM following exposure to variable RH were examined as displayed in Fig. 2b. It was found that the absorbance of the hybrid NFM lying in the range of 410–550 nm corresponds to the spectral characteristics of $CoCl_2{\cdot}6H_2O$ [7]. Similarly, there is a weak absorption bands located at 580–750 nm (yellow and red light) with absorbance peak at ~670 nm, which may be caused by a small amount of residual anhydrous cobalt chloride inside the fibers. As the humidity decreases, the absorption bands of 580–750 nm are gradually sharpening, which correspond to the pink faded and turn to blue by degrees. Until 12.4% RH, the absorbing peak from 410 to 550 nm of the NFM disappears, and the absorption peak of 710 nm reaches a maximum value, which corresponds to the spectral characteristics of anhydrous $CoCl_2$ [7]. It suggests that in different RH, the PA66/$CoCl_2{\cdot}6H_2O$ NFM shows different colors, indicating the composite NFM have potential application in humidity visualization hygrometer.

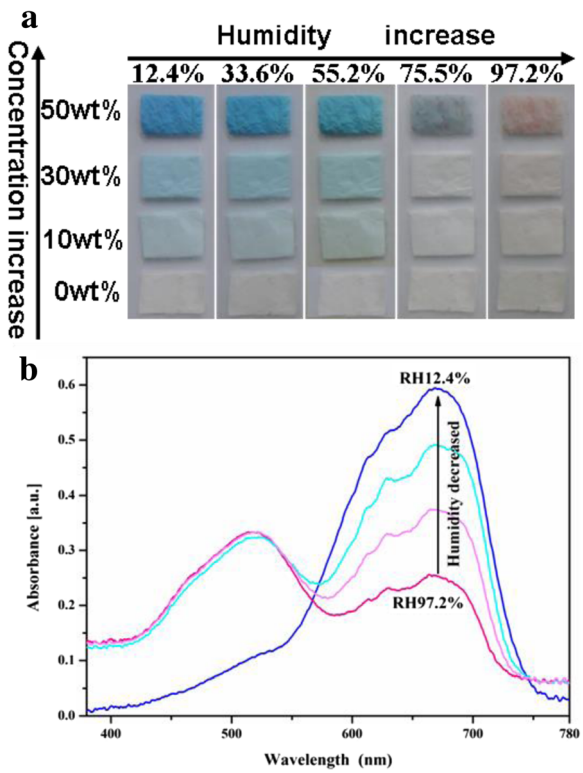

Fig. 2 **a** The photographs of PA66/$CoCl_2{\cdot}6H_2O$ NFMs containing different concentrations of $CoCl_2{\cdot}6H_2O$: 0, 10, 30, and 50 wt% in different RH. **b** Humidity dependence of visible absorption spectra (380–780 nm) of PA66/$CoCl_2{\cdot}6H_2O$ (50 wt%)

Humidity Sensing Characteristics by QCM

Sensors based on QCM technique has been attracted a lot of interests due to its advantages of high sensitivity and reliability [14, 23, 24]. The operating principle of these sensors is primarily associated with the adsorption of the water molecules on the surface of the QCM electrode, inducing variation in the molar response of a quartz crystal, which lead to the resonance frequency shift [14, 25]. Consequently, we also selected QCM for further humidity sensitivity measurement.

Sensitivity

Figure 3 shows the QCM frequency response curves of PA66/$CoCl_2$ NFMs with different concentrations of $CoCl_2$ under different RH. As can be found that the resonant frequency of the pure PA66 NFM did not show obvious change even at 97.2% RH, revealing that pure PA66 NFM was weakly sensitive to humidity. In contrast, the resonant frequency of the PA66 mixed with cobalt chloride NFMs sensors obviously shifted. The resonant frequencies of all the three sensors were negative growth corresponded to

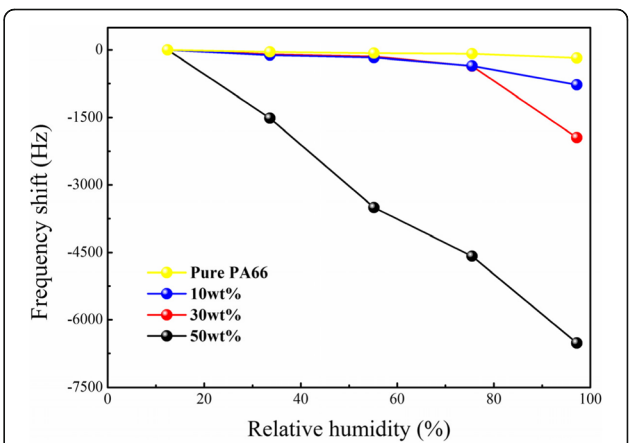

Fig. 3 The relationship between the frequency shift and the corresponding relative humidity at different concentration of $CoCl_2{\cdot}6H_2O$ on PA66 NFMs measured by humidity ascending mode

the increasing of humidity. The frequency shifts of the PA66/$CoCl_2$·$6H_2O$ (10 wt%) NFM sensor and the PA66/$CoCl_2$·$6H_2O$ (30 wt%) NFM sensor are very close and increased slowly below 75.5% RH. After exceeded 75.5% RH, the frequency shifts of the 10 and 30 wt% NFM sensors increased in a steep manner, which maybe due to that the complexes (Co) shielded by the PA66 molecular chain in low-RH regions and liberated in the high hydrated state in the high RH region [26]. And at 97.2% RH, the maximum frequency shifts were −777 and −1944 Hz for 10 and 30 wt% NFM sensors, respectively. As the concentration of $CoCl_2$·$6H_2O$ further increased, the shielding effect was weakened; consequently, the resonant frequency shift of the 50 wt% NFM sensor was linear negative increase with the increase of RH and its regression coefficient R^2 reached 0.9937. Its maximum frequency shift was −6519.5 Hz at 97.2% RH. The results indicating that incorporation of cobalt chloride can increase the humidity sensitive of the QCM-based NFMs sensors and the sensing response increased with increasing concentration of cobalt chloride in the NFMs, and there were more absorption sites [10, 27] on the NFM due to the higher concentration of $CoCl_2$ which increased the total amount of absorption water molecules. Based on this discovery, the future investigations about coating CoCl2 on PA66 nanofibers using the modified coaxial and triaxial electrospinning processes are worthy of conducting [28–31].

Repeatability and Humidity Hysteresis Characteristic

It is well known that response and recovery behavior is an important characteristic for evaluating the performance of humidity sensors which corresponding to the water molecule adsorption and desorption processes [32]. Moreover, sensor repeatability refers to the successive runs using a single sensor to evaluate discrepancies in its response [33]. To investigate this performance, the PA66/$CoCl_2$·$6H_2O$ NFM humidity sensors were alternately placed into different humidity bottles. The response and recovery characteristic curves for one cycle from three humidity differences: 12.4–55.2% RH, 12.4–75.5% RH, and 12.4–97.2% RH, with the PA66/$CoCl_2$·$6H_2O$ (10, 30, and 50 wt%) NFMs QCM sensors were shown in Additional file 1: Figure S1 and Table S1. To investigate the sensors' repeatability, the sensors were tested in two fixed humidity levels repeatedly. In this test, the PA66/$CoCl_2$·$6H_2O$ (50 wt%) NFM sensors' repeatability was tested in three humidity differences which corresponded to 12.4–55.2% RH, 12.4–75.5% RH, and 12.4–97.2% RH for five cycles showed as a representative (Fig. 4a–c). In these three conditions, whenever the sensor was switched to a humidity condition, the frequency promptly changed and rapidly reached a relative stable value, which was very close to the original value. Each cycle had a similar curved shape, and each stable value was very close. It suggests that the PA66/$CoCl_2$·$6H_2O$

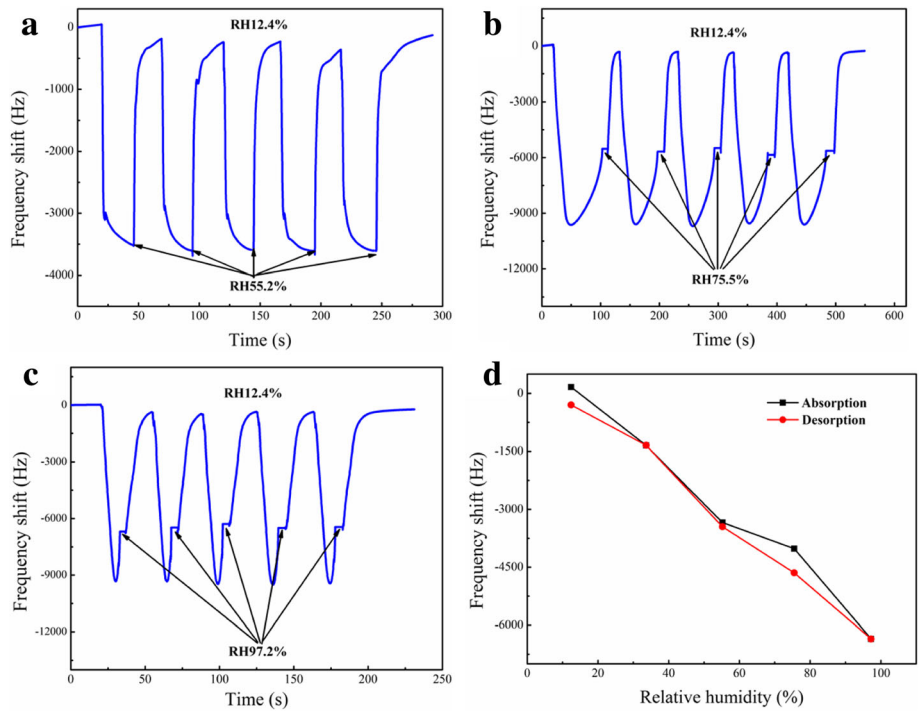

Fig. 4 The repeatability characteristic curves of QCM-based PA66/$CoCl_2$·$6H_2O$ (50 wt%) NFM sensor for 5 cycles of RH adsorption–desorption **a** between 12.4 and 55.2% RH, **b** between 12.4 and 75.5% RH, and **c** between 12.4 and 97.2% RH. **d** Humidity hysteresis characteristic of QCM-based PA66/$CoCl_2$·$6H_2O$ (50 wt%) NFM sensor

NFM sensors have good reproducibility in different humidity differences for humidity sensing.

Sensor hysteresis is examined to obtain some information about the reliability [14, 34]. Figure 4d shows the PA66/$CoCl_2{\cdot}6H_2O$ (50 wt%) NFM sensors' humidity hysteresis characteristic. The black line in the figure was measured from low RH to high RH (from 12.4 to 97.2%), i.e., for the adsorption process, and the red line represents desorption process (measured in the opposite direction). The curves between adsorption process and desorption process have good coincidence for the as-spun sensor. The maximum humidity hysteresis was 9.9% (at about 75.5% RH) for PA66/$CoCl_2{\cdot}6H_2O$ NFM sensor with concentration of 50 wt% $CoCl_2{\cdot}6H_2O$, indicating a good reliability of these humidity sensors, and the other humidity hysteresis curves of electrospun PA66/$CoCl_2{\cdot}6H_2O$ NFM with different $CoCl_2{\cdot}6H_2O$ concentration were shown in Additional file 1: Figure S2. Moreover, the stability of the sensor was also examined showing in Additional file 1: Figure S3.

Morphology of the As-Spun Membranes

As mentioned in the background, the high humidity sensitivity of electrospun PA66/$CoCl_2{\cdot}6H_2O$ NFM may due to their microstructures. Consequently, the SEM and TEM images of the as-spun NFMs samples are examined. As displayed in Fig. 5, these SEM images indicate that all of these NFMs with different concentrations of $CoCl_2{\cdot}6H_2O$ were the form of nonwoven mats with randomly oriented fibers. Figure 5a shows PA66 fibers have a relatively uniform diameter of about 100 nm. As showed in Fig. 5b, the diameter distribution of PA66/$CoCl_2{\cdot}6H_2O$ (10 wt%) fibers was about 100 to 500 nm. This might due to the increase of the solution conductivity leading to the increase of the solution-jet instability in the electric field [35]. In addition, in Fig. 5b, we found some smaller diameter (about 25 nm) nanofibers, namely, spider-net-like structure, which was shown in the inset of Fig. 5b more clearly. The formation of the spider-net-like structure may be due to the increased ionization of the polymer solution in the presence of cobalt ions (Co^{2+}) and chloride ions (Cl^-) during electrospinning process. Formic acid, a polar monoprotic solvent with high dielectric constant, is capable of attacking the lactam of nylon to produce a series of short chain oligomer/monomer ions (–$CONH^{2+}$–) [36]. The Cl^- and Co^{2+} could further increase the concentration of ions in the electrospinning solution. The increased of ions could initiate the splitting up of subnanofibers from the main fibers and form the spider-net-like structure during electrospinning [37]. The PA66/$CoCl_2{\cdot}6H_2O$ (30 wt%) fibers were relatively uniform with a diameter of about 100 nm (Fig. 5c). Figure 5d shows the surface morphology of PA66/$CoCl_2{\cdot}6H_2O$ (50 wt%) NFM. The further increased in the $CoCl_2{\cdot}6H_2O$ (50 wt%) concentration led to a fiber-sticking structure which is more clearly showed in the inset of Fig. 5d. This fiber morphology could be caused by the localized charge effects on the surface of the fibers and slow evaporation of solvent from the fibers [38, 39].

Figure 6 shows the TEM images of the PA66/$CoCl_2{\cdot}6H_2O$ (50 wt%) fibers. From Fig. 6a and its partial enlarged view Fig. 6b, we could see aggregated cobalt

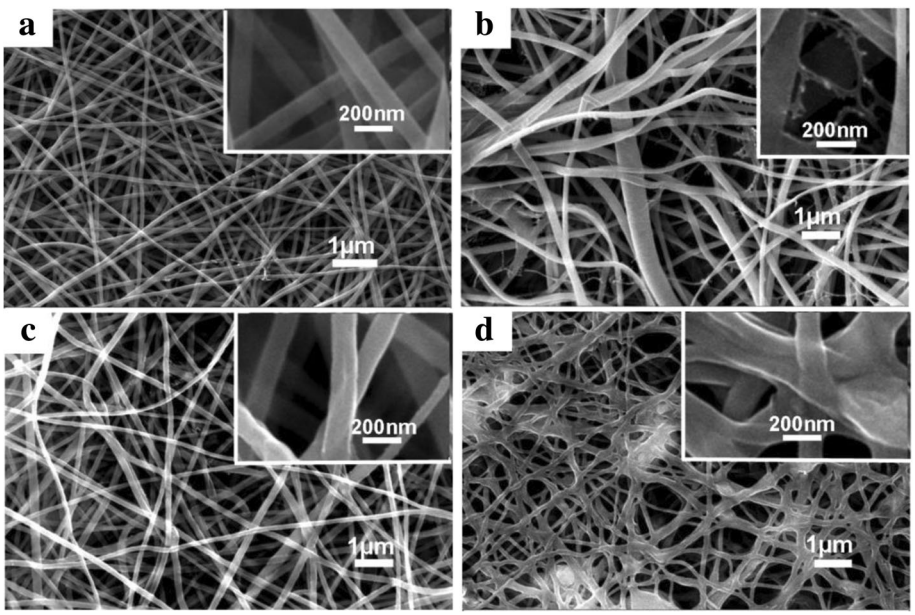

Fig. 5 SEM images of **a** pure PA66 NFM, **b** PA66/$CoCl_2{\cdot}6H_2O$ (10 wt%) NFM, **c** PA66/$CoCl_2{\cdot}6H_2O$ (30 wt%) NFM, and **d** PA66/$CoCl_2{\cdot}6H_2O$ (50 wt%) NFM

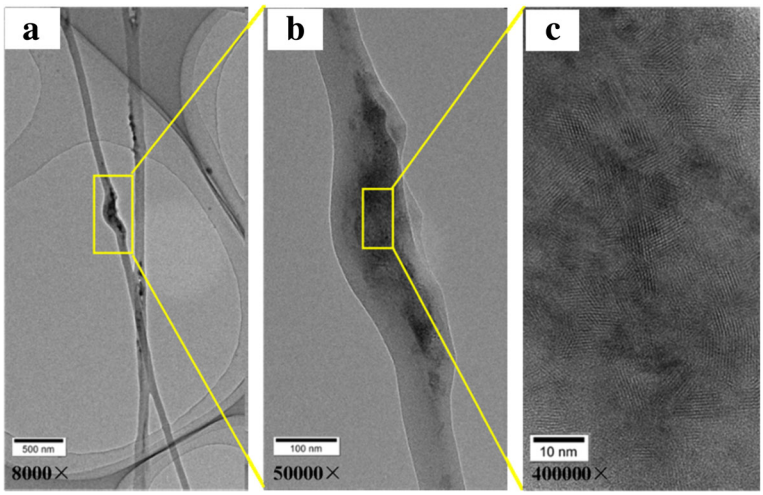

Fig. 6 TEM images of PA66/$CoCl_2$·$6H_2O$ (50 wt%) fibers: **a** magnified 8000 times and **b** magnified 50000 times. **c** HRTEM image of cobalt chloride particles

chloride particles dispersed in the PA66 nanofibers. Figure 6c is the high-resolution TEM (HRTEM) image of the cobalt chloride particles. From this image, a lot of lattice stripes with grain size of nearly 6 nm assigned to the crystalline cobalt chloride were observed. On the other hand, some regions were not lattice stripes, suggesting that partial cobalt chloride has an amorphous structure.

FT-IR Spectra and Humidity Sensing Mechanism

Figure 7 shows the FT-IR spectra of the pure PA66 NFM and the PA66/$CoCl_2$·$6H_2O$ (50 wt%) NFM in the dry and hydrated states. Comparing the spectra in dry and hydrated states, there are two obvious absorption bands located at 430–900 and 2750–3660 cm^{-1} in the dehydration curve. The absorption bands at 430–900 cm^{-1} are attributed to the bending and rocking modes of Co–OH_2 (cobalt-water bond) and the rocking mode of O–H···Cl (hydrogen bonding with chlorine). The bands at 2750–3660 cm^{-1} correspond to the stretching mode of Co–OH_2 [40, 41]. It indicates that the cobalt chloride in NFM lost crystalline water in low humidity and absorbed crystalline water in high humidity. In contrast, there is a pronounced peak at about 1600 cm^{-1} in the dry state, which cannot found in the hydrated state spectrum as well as the pure PA66 spectrum. It seems that the addition of $CoCl_2$ in PA66 membrane could lead to the formation of coordination bonds between Co ions and PA66 molecular chain (probably the peptide groups), which caused the 1600 cm^{-1} peak in the dry PA66/$CoCl_2$ NFM; as the NFM adsorbed water molecules, these coordination bonds are gradually destroyed so that this peak disappears in the hydrated NFM [26].

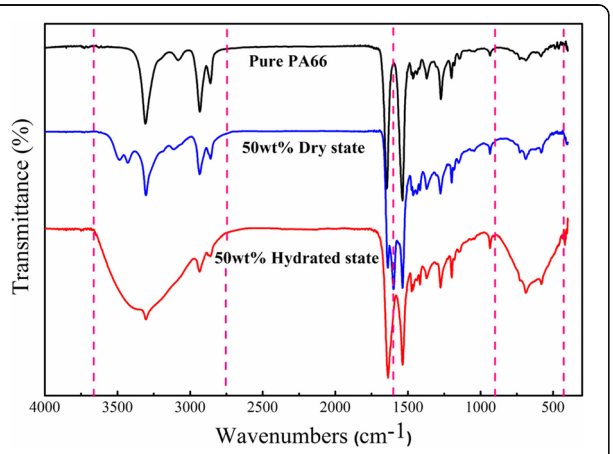

Fig. 7 FT-IR spectra of pure PA66 NFM and PA66/$CoCl_2$·$6H_2O$ (50 wt%) NFM in dry and hydrated states

The humidity sensitive characteristics of the hybrid PA66/cobalt chloride NFMs mainly come from the cobalt chloride. When exposed to dry atmosphere, the cobalt chloride loses its crystalline water, conversely, in a wet environment it absorbs water molecules and turns into hydrated cobalt chloride. In this process, the color of PA66/cobalt chloride NFM changes. Moreover, in the process of dehydration and hygroscopic, the mass of the NFMs also changes, which leads to an according change of resonant frequency. In addition, it is noted that the PA66 has very small contribution to the mass change because the pure PA66 NMF can only cause a small frequency shift when RH changes.

Conclusions

In summary, hybrid PA66/cobalt chloride humidity sensitive colorimetric nanofibrous membranes have been fabricated successfully by electrospinning. The influences of $CoCl_2$ concentrations on morphology, color, and humidity

sensitivity of the NFMs have also been systematically studied. The hybrid membranes exhibit different colors in different humidity conditions, indicating that PA66/cobalt chloride NFMs have promising application in visual hygrometer. Furthermore, PA66/cobalt chloride NFMs deposited on QCM also exhibit interesting humidity sensing properties. Since the nanofibrous structure may increase the sensing area and surface activity, the QCM-based humidity sensor shows high sensitivity, fast response, and recovery time, good reproducibility in moisture-sensitive and longtime stability in a stable humidity environment with a little frequency shift. These results indicate that the PA66/cobalt chloride NFM sensor has potential applications in humidity detection.

Additional file

Additional file 1: Supporting information. (DOC 475 kb)

Acknowledgements
This work was supported by the National Natural Science Foundation of China (51373082 and 51673103), the Taishan Scholars Programme of Shandong Province, China (ts20120528), the Shandong provincial key research and development plan (2016GGX102011), the Shandong Provincial Natural Science Foundation, China (ZR2016EMB09), and the Research Fund for the Doctoral Program of Higher Education of China (20133706110004).

Authors' Contributions
MHY, XY, and YZL designed the experiments. MHY, XY, and XXH prepared the colorful NFMs. MHY, XY, and XXW collected and analyzed the data of the scanning electron microscopy, transmission electron microscope, and color measurement. MHY and JZ collected and analyzed the QCM humidity characteristics. JZ, MY, and XN analyzed the IR spectra data and absorption spectra. All authors read and approved the final manuscript.

Competing Interests
The authors declare that they have no competing interests.

Publisher's Note

Author details
[1]Collaborative Innovation Center for Nanomaterials & Devices, College of Physics, Qingdao University, Qingdao 266071, China. [2]Industrial Research Institute of Nonwovens & Technical Textiles, College of Textiles & Clothing, Qingdao University, Qingdao 266071, China. [3]Department of Mechanical Engineering, Columbia University, New York, NY 10027, USA.

Received: 12 April 2017 Accepted: 11 May 2017
Published online: 19 May 2017

References
1. Xia L, Li LC, Li W, Kou T, Liu DM (2013) Novel optical fiber humidity sensor based on a no-core fiber structure. Sensors Actuators A 190:1–5
2. Karimov KS, Qazi I, Khan TA, Draper PH, Khalid FA, Mahroof-Tahir M (2008) Humidity and illumination organic semiconductor copper phthalocyanine sensor for environmental monitoring. Environ Monit Assess 141:323–328
3. Liu WT, Niiler PP (1984) Determination of monthly mean humidity in the atmosphere surface layer over oceans from satellite date. J Phys Oceanogr 14:1451–1457
4. Yu HH, Cao T, Zhou LD, Gu ED, Yu DS, Jiang DS (2006) Layer-by-Layer assembly and humidity sensitive behavior of poly(ethyleneimine)/multiwall carbon nanotube composite films. Sensors Actuators B 119:512–515
5. Gu L, Huang QA, Qin M (2004) A novel capacitive-type humidity sensor using CMOS fabricationtechnology. Sensors Actuators B 99:491–498
6. Lee SP, Park KJ (1996) Humidity sensitive field effect transistors. Sensors Actuators B 35:80–84
7. Tsigara A, Mountrichas G, Gatsouli K, Nichelatti A, Pispas S, Madamopoulos N, Vainos NA, Du HL, Roubani-Kalantzopoulou F (2007) Hybrid polymer/cobalt chloride humidity sensors based on optical diffraction. Sensors Actuators B 120:481–486
8. Tian ET, Wang JX, Zheng YM, Song YL, Jiang L, Zhu DB (2008) Colorful humidity sensitive photonic crystal hydrogel. J Mater Chem 18:1053–1160
9. Hawkeye MM, Brett MJ (2011) Optimized colorimetric photonic-crystal humidity sensor fabricated using glancing angle deposition. Adv Funct Mater 21:3652–3658
10. Steyaert I, Rahier H, Clerck KD (2015) Nanofibre-based sensors for visual and optical monitoring. Nanosci Technol 96:157–177
11. Benvidi A, Nafar MT, Jahanbani S, Tezerjani MD, Rezaeinasab M, Dalirnasab S (2017) Developing an electrochemical sensor based on a carbon paste electrode modified with nano-composite of reduced graphene oxide and CuFe2O4 nanoparticles for determination of hydrogen peroxide. Mater Sci Eng C 75:1435–1447
12. Han L, Yang DP, Liu A (2015) Leaf-templated synthesis of 3D hierarchical porous cobalt oxide nanostructure as direct electrochemical biosensing interface with enhanced electrocatalysis. Biosens Bioelectron 63:145–152
13. Mahmoudi N, Simchi A (2017) On the biological performance of graphene oxide-modified chitosan/polyvinyl pyrrolidone nanocomposite membranes: In vitro and in vivo effects of graphene oxide. Mater Sci Eng C 70:121–131
14. Wang XF, Ding B, Yu JY, Wang MR (2011) Highly sensitive humidity sensors based on electro-spinning/netting a polyamide 6 nano-fiber/net modified by polyethyleneimine. J Mater Chem 21:16231–16238
15. Wang W, Li ZY, Liu L, Zhang HN, Zheng W, Wang Y, Huang HM, Wang ZJ, Wang C (2009) Humidity sensor based on LiCl-doped ZnO electrospun nanofibers. Sensors Actuators B 141:404–409
16. Azmer MI, Zafar Q, Ahmad Z, Sulaiman K (2016) Humidity sensor based on electrospun MEH-PPV: PVP microstructured composite. RSC Adv 6(42): 35387–35393
17. Pascariu P, Airinei A, Olaru N, Petrila I, Nica V, Sacarescu L, Tudorache F (2016) Microstructure, electrical and humidity sensor properties of electrospun NiO–SnO2 nanofibers. Sensors Actuators B Chem 222:1024–1031
18. Yin SN, Wang CF, Liu SS, Chen S (2013) Facile fabrication of tunable colloidal photonic crystal hydrogel supraballs toward a colorimetric humidity sensor. J Mater Chem C 1:4685–4690
19. Kim E, Kim SY, Jo G, Kim S, Park MJ (2012) Colorimetric and resistive polymer electrolyte thin films for realtime humidity sensors. ACS Appl Mater Interfaces 4:5179–5187
20. Saha A, Tanaka Y, Han Y, Bastiaansen CMW, Broer DJ, Sijbesma RP (2012) Irreversible visual sensing of humidity using a cholesteric liquid crystalwz. Chem Commun 48:4579–4581
21. Huang W, Jiang Y, Li X, Li XJ, Wang JY, Wu Q, Liu XK (2013) Solvothermal synthesis of microporous, crystalline covalent organic framework nanofibers and their colorimetric nanohybrid structures. ACS Appl Mater Interfaces 5: 8845–8849
22. Kharaz A, Jones BE (1995) A distributed optical-fiber sensing system for multi-point humidity measurement. Sensors Actuators A 47:491–493
23. Yoshikawa C, Qiu J, Shimizu Y, Huang CF, Gelling OJ, Bosch EVD (2017) Concentrated polymer brush-Concentrated polymer brushmodified silica particle coating confers biofouling-resistance on modified materials. Mater Sci Eng C 70:272–277
24. Zhou Z, Rajabzadeh S, Fang L, Miyoshi T, Kakihana Y, Matsuyama H (2017) Preparation of robust braid-reinforced poly(vinyl chloride) ultrafiltration hollow fiber membrane with antifouling surface and application to filtration of activated sludge solution. Mater Sci Eng C 77:662–671
25. Zhang HD, Yan X, Zhang ZH, Yu GF, Han WP, Zhang JC, Long YZ (2016) Electrospun PEDOT:PSS/PVP nanofibers for CO gas sensing with quartz crystal microbalance technique. Int J Polymer Sci 2016
26. Otsuki S, Adachi K (1993) Humidity dependence of visible absorption spectrum of gelatin films containing cobalt chloride. J Appl Polym Sci 48: 1557–1564
27. Ding B, Kim J, Miyazaki Y, Shiratori S (2004) Electrospun nanofibrous membranes coated quartz crystal microbalance as gas sensor for NH3 detection. Sensors Actuators B 101:373–380

28. Wen HF, Yang C, Yu DG, Li XY, Zhang DF (2016) Electrospun zein nanoribbons for treatment of lead-contained wastewater. Chem Eng J 290: 263–272
29. Yang C, Yu DG, Pan D, Liu XK, Wang X, Annie Bligh SW, Williams GR (2016) Electrospun pH-sensitive core–shell polymer nanocomposites fabricated using a tri-axial process. Acta Biomater 35:77–86
30. Yang GZ, Li JJ, Yu DG, He MF, Yang JH, Williams GR (2017) Nanosized sustained-release drug depots fabricated using modified tri-axial electrospinning. Acta Biomater 53:233–241
31. Park CK, Xue RP, Lannutti JJ, Farson DF (2016) Ablation characteristics of electrospun core-shell nanofiber by femtosecond laser. Mater Sci Eng C 65: 232–239
32. Qi Q, Zhang T, Yu QJ, Wang R, Zeng Y, Liu L, Yang HB (2008) Properties of humidity sensing ZnO nanorods-base sensor fabricated by screen-printing. Sensors Actuators B 133:638–643
33. Gao F, Tang LJ, Dai L, Wang L (2007) A fluorescence ratiometric nano-pH sensor based on dual-fluorophore-doped silica nanoparticles. Spectrochim Acta A 67:517–521
34. Xu L, Wang R, Xiao Q, Zhang D, Liu Y (2011) Micro humidity sensor with high sensitivity and quick response/recovery based on ZnO/TiO2 composite nanofibers. Chin Phys Lett 28(7):070702
35. Fridrikh SV, Yu JH, Brenner MP, Rutledge GC (2003) Controlling the fiber diameter during electrospinning. Phys Rev Lett 90:144502
36. Schaefgen JR, Trivisonno CF (1951) Polyelectrolyte behavior of polyamides. I. Viscosities of solutions of linear polyamides in formic acid and sulfuric acid. J Am Chem Soc 73:4580–4585
37. Pant HR, Bajgai MP, Nam KT, Seo YA, Pandeya DR, Hong ST, Kim HY (2011) Electrospun nylon-6 spider-net like nanofiber mat containing TiO2 nanoparticles: A multifunctional nanocomposite textile material. J Hazard Mater 185:124–130
38. Wang XF, Ding B, Yu JY, Si Y, Yang SB, Sun G (2011) Electro-netting: Fabrication of two-dimensional nano-nets for highly sensitive trimethylamine sensing. Nanoscale 3:911–915
39. Patel AC, Li SX, Wang C, Zhang WJ, Wei Y (2007) Electrospinning of porous silica nanofibers containing silver nanoparticles for catalytic applications. Chem Mater 19:1231–1238
40. Gamo I (1961) Infrared spectra of water of crystallization in some inorganic chlorides and sulfates. Bull Chem Soc Jpn 34:760–764
41. Augsburger MS, Strasser E, Perino E, Mercader RC, Pedregosa JC (1998) FTIR and mössbauer investigation of a substituted palygorskite: Silicate with a channel structure. J Phys Chem Solids 59:175–180